Characteristics of a Titanium-oxide Layer Prepared by Plasma Electrolytic Oxidation for Hydrogen-ion Sensing

Do Kyung Lee[1], Deok Rok Hwang[1], and Young-Soo Sohn[2,+]

Abstract

The characteristics of a titanium oxide layer prepared using a plasma electrolytic oxidation (PEO) process were investigated, using an extended gate ion sensitive field effect transistor (EG-ISFET) to confirm the layer's capability to react with hydrogen ions. The surface morphology and element distribution of the PEO-processed titanium oxide were observed and analyzed using field-emission scanning-electron microscopy (FE-SEM) and energy-distribution spectroscopy (EDS). The titanium oxide prepared by the PEO process was utilized as a hydrogen-ion sensing membrane and an extended gate insulator. A commercially available n-channel enhancement MOSFET (metal-oxide-semiconductor FET) played a role as a transducer. The responses of the PEO-processed titanium oxide to different pH solutions were analyzed. The output drain current was linearly related to the pH solutions in the range of pH 4 to pH 12. It was confirmed that the titanium-oxide layer prepared by the PEO process could feasibly be used as a hydrogen-ion-sensing membrane for EGFET measurements.

Keywords: Titanium oxide, Plasma electrolytic oxidation, Extended gate field effect transistor, Hydrogen ion sensing

1. INTRODUCTION

Almost half a century ago, P. Bergveld suggested a new ion-measurement technique based on a combined MOSFET (metal-oxide-semiconductor field-effect-transistor) and a glass electrode detection principle [1]. These ion-sensitive solid-state devices were called ISFETs (ion-sensitive FETs). Since then, these FET-type sensors have evolved, not only for ion measurements, but also for biological or physiological measurements [2-6]. In addition, the structures were also modified from a planar FET type to extended-gate FETs (EGFETs) and nanowire FETs. The diverse materials for FET-type sensors have been studied, from silicon to carbon-based, including graphene [7-13].

Plasma electrolytic oxidation (PEO) treatments for light metals have been known for decades and have been established with well-known industrial surface treatments. Recently, PEO coatings have been investigated to overcome their inherent shortcomings, e.g., porosity and the limited extent of the PEO-layer composition, by introducing particles into the electrolytes during growth in order to seal defects and improve the formation range and function of the produced layers [14-17].

Titanium (Ti), known as the ninth earth-abundant material, and its alloys have attracted considerable interest due to their high strength-to-weight ratio, high corrosion and wear resistance, and biocompatibility [18, 19]. In addition, Ti and its alloys have been considered for use in PEO coatings to improve the coatings' properties [14, 16-20]. Among various pH sensing membranes such as silicon oxide, silicon nitride, aluminum oxide, tantalum oxide, titanium oxide is also used for ISFET or EGFET sensing membranes [5, 21].

In this study, a titanium-oxide layer was prepared using the PEO process, and its surface characteristics, including surface morphology and element distribution were observed and analyzed. The feasibility of this thin layer as both a hydrogen-ion-sensing membrane and an extended gate insulator was investigated using a commercially available n-channel enhancement MOSFET.

2. EXPERIMENTAL DETAILS

A Ti substrate with dimensions of 20 mm × 20 mm × 1 mm was used as the anode for the PEO treatment. Afterwards, the specimens

[1]Department of Advanced Material Science and Chemical Engineering, Daegu Catholic University, 13-13 Hayang-ro, Hayang-eup, Gyeongsan-si, Gyeongbuk, 38430 Republic of Korea.
[2]Department of Biomedical Engineering, Daegu Catholic University, 13-13 Hayang-ro, Hayang-eup, Gyeongsan-si, Gyeongbuk, 38430 Republic of Korea.
+Corresponding author: sohnys@cu.ac.kr

were cleaned sequentially with a neutral detergent, ultrasonication for 15 minutes in acetone, and 15 minutes in distilled water. The specimens were rinsed and then dried. The PEO treatment was carried out for 10 seconds in a bath made of stainless steel that served as the cathode while applying a 160 V voltage. The electrolytes used in this study contain KOH, Na_3PO_4, and Na_2SiO_3. The detailed quantities of the electrolyte composition are listed in Table 1. After the PEO treatment, the specimens were rinsed with distilled water and dried.

Table 1. Electrolyte composition

| KOH (g/L)	Na_3PO_4 (g/L)	Na_2SiO_3 (g/L)
10	4	12

A surface observation of the PEO-treated specimen was carried out using field-emission scanning-electron microscopy (FE-SEM: Hitach S-4800, Japan). The elemental composition of the PEO-treated specimen was investigated by energy-distribution spectroscopy (EDS: HORIBA X-Max, Japan).

For the pH measurement, the PEO-processed titanium-oxide layer played roles as a sensing membrane and an extended gate insulator. A commercially available n-channel enhancement MOSFET (2N7008) was used as a transducer. A standard pH solution (Duksan, Korea) was used for the measurement. A reference electrode (Ag / AgCl filled with KCl) was used for the electrical measurement, and a semiconductor device analyzer (Elecs EL-423, Korea) was used to obtain a graph of the drain voltage (V_d) versus the drain current (I_d). The specimen was inserted into a corrosion-test cell, and the exposed area was a 1-cm-diameter circle. Figure 1 shows the schematic diagram of the electrical-measurement setup (Fig. 1(a)), and the reference electrode, specimens, and corrosion-test cell (Fig. 1(b)).

3. RESULTS AND DISCUSSION

Figure 2 shows an FE-SEM micrograph of the surface of the PEO coating prepared by electrolytes whose composition is listed in Table 1. It is hard to find holes in the coating as shown in Fig. 2(a), and when the image was magnified 30 times as shown in Fig. 2(b), it can be seen that the size of the pores is less than 200 nm (scale bars are different between Figs. 2(a) and (b).). This relatively dense coating can be attributed to the introduction of
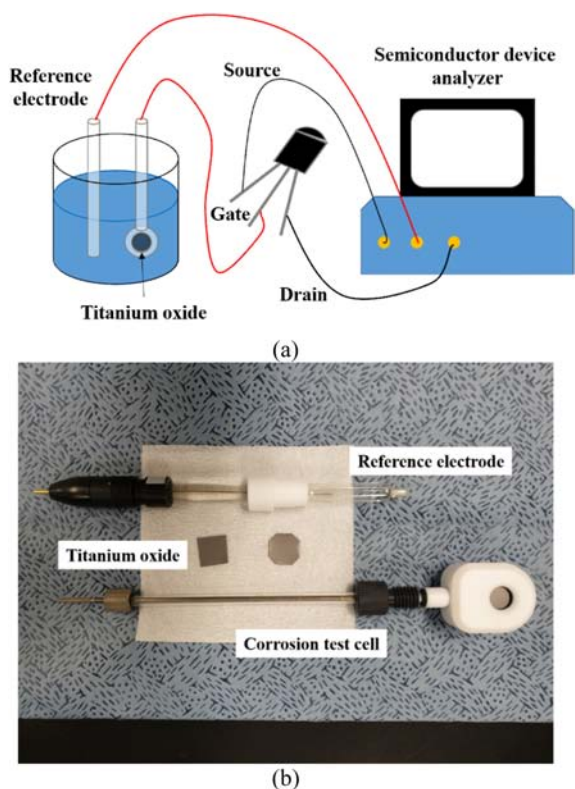
Fig. 1. (a) Schematic diagram of electrical measurement setup; (b) reference electrode, specimens, and corrosion-test cell.
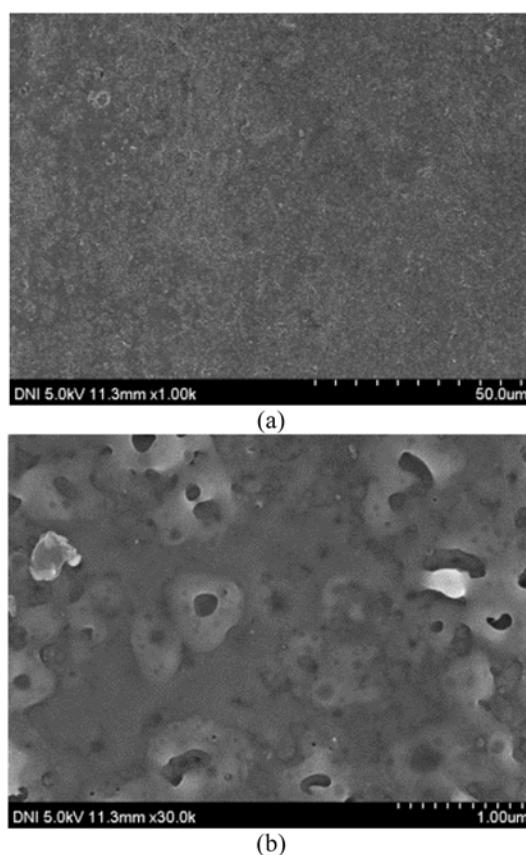
Fig. 2. FE-SEM micrograph of the surface of the PEO coating. (a) 1k magnified image; (b) 30k magnified image.

particles into the electrolytes [14-17]. The cross section of the PEO-processed titanium-oxide layer is shown in Fig. 3. An examination of the coatings, formed with the above mentioned process and the electrolyte composition listed in Table 1, revealed that the average thickness of the layer was 257.8 nm. The average thickness was calculated from the thickness examination of SEM images for the 4 sections of the specimen.
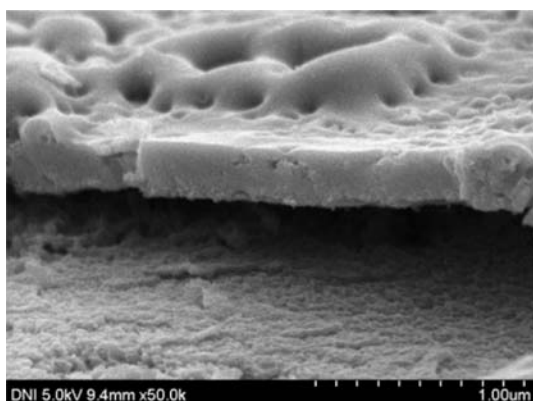

Fig. 3. Cross section of the SEM image of the specimen.

Table 2 lists the elemental composition of the PEO coatings using EDS. Element symbols O, Si, and P represent oxygen, silicon, and phosphorus, respectively. Figure 4 shows the EDS spectrum of the PEO coating, which shows two main Ti and O peaks. According to the EDS analysis, Ti and O are the main elements of the coated layer. Looking closely at the atomic-percentage ratio of the elemental composition of the PEO coating, it can be seen that the ratio of Ti to O is very close to 1:2. Therefore, the dense titanium-oxide layer was well formed with the PEO process.

Table 2. EDS analysis of the PEO layer.

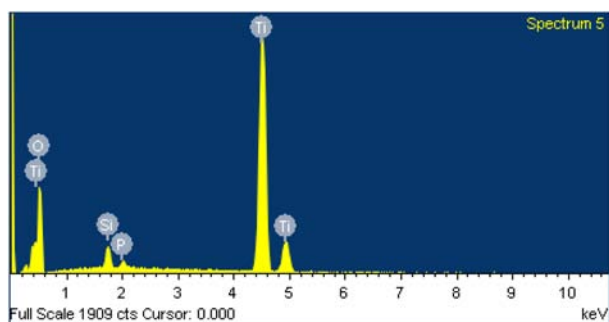| Element	O	Si	P	Ti
Weight%	41.44	1.64	0.53	56.39
Atomic%	67.40	1.52	0.45	30.63

Fig. 4. EDS spectrum of the PEO coating.

The pH is strongly related to the hydrogen-ion concentration; a lower pH value has a higher concentration of hydrogen ions. From the site-binding model, higher positive ions are adsorbed onto the titanium-oxide layer at equilibrium in the lower pH solution, which is equivalent to applying a positive voltage to the gate of the FETs [5].

Figure 5 shows the I_d - V_d graphs of the commercial n-MOSFET(2N7008) and the EGFET with five different pH solutions (pH 2, pH 4, pH 7, pH 10, and pH 12) with 4.0 V voltage applied to the reference electrode. In this study, an n-channel enhancement MOSFET was utilized. Figure 5(a) shows the I_d - V_d characteristic of the commercial n-MOSFET(2N7008). As gate voltage (V_g) increased, the I_d increased, and the I_d started to flow the channel by applying gate voltage higher than 1.5 V. This graph demonstrated that 2N7008 is n-channel enhancement MOSFET. Higher concentrations of positive hydrogen ions in a lower pH solution could induce a higher concentration of electrons in the n-channel of the FET(2N7008). Thus, I_d increases
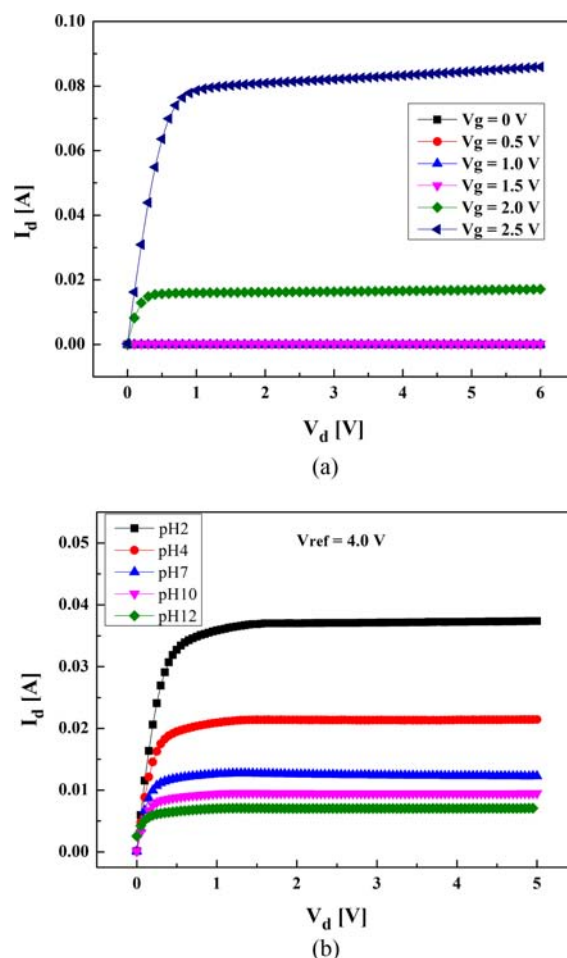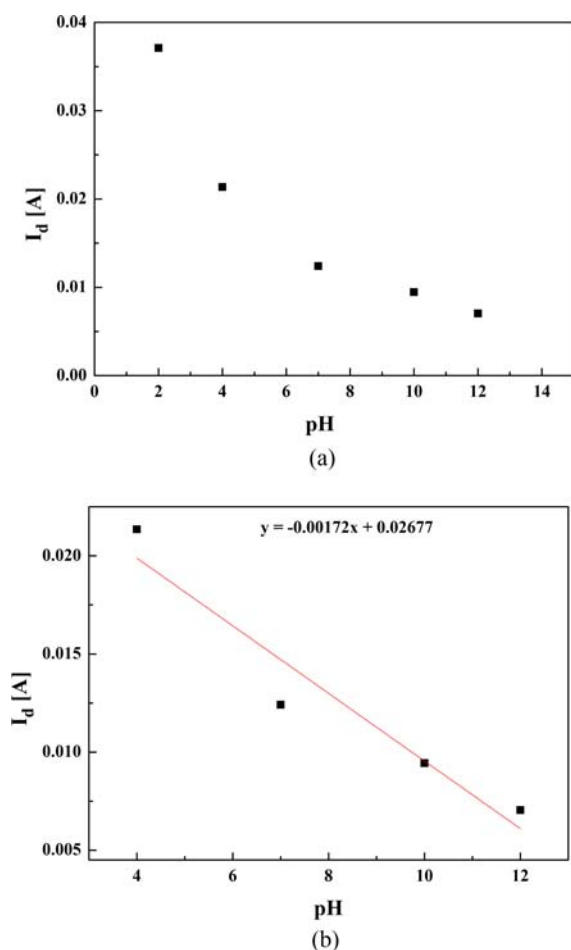

(a)

(b)

Fig. 5. I_d-V_d graphs of (a) the commercial n-MOSFET(2N7008) and (b) the EGFET with different pH values.

with decreasing the value of pH solutions in the saturation region, as shown in Fig. 5(b). In the saturation region on the I_d - V_d graph, I_d is related to the square of the V_g [22]. It can be seen that the difference in I_d between the solutions increases as the value of the pH solution decreases in the saturated region. Since the saturation region starts approximately at $V_d = 1.5$ V, I_d at $V_d = 3$V was selected to investigate the relation between I_d and the pH values.

Figure 6(a) shows the pH versus I_d in the saturated region. The response of the titanium-oxide-based EGFET to pH 2 was quite high. Thus, the relations were investigated without the pH 2 output. From the linear regression line, the relation between I_d in the saturated region and the pH solutions from pH 4 to pH 12 was linear, as shown in Fig. 6(b). The sensitivity, the slope of the linear regression line is -1.72 mA/pH in the range of pH 4 to pH 12. The correlation coefficient was 96.4%, which implies that the output was quite linear to the pH solutions, from pH 4 to pH 12. In this study, the titanium-oxide layer formed using the PEO process could feasibly be used as a hydrogen-ion-sensing membrane for

EGFET measurements. Further research is still needed to determine the for optimized conditions for film growth to detect various ions.

4. CONCLUSIONS

A titanium oxide layer was prepared using the PEO process, and its surface characteristics, including surface morphology and element distribution were observed and analyzed. The surface was densely coated during the PEO process. This could be attributed to the introduction of particles into the electrolytes.

According to the EDS analysis, Ti and O were the main elements of the coated layer, and the ratio of Ti to O was very close to 1:2. The gating effect of the adsorbed positive hydrogen-ion concentrations on the titanium-oxide layer modulated I_d. I_d increased with the decreasing pH in the saturation region. From the linear regression analysis, the relation between I_d in the saturated region and the pH solutions from pH 4 to pH 12 was linear. The feasibility of this thin layer as an ion-sensing membrane and an extended gate insulator was confirmed.

ACKNOWLEDGMENT

(a)

$y = -0.00172x + 0.02677$

(b)

Fig. 6. (a) pH versus I_d in the saturated region; (b) linear regression of the relation between I_d and pH from 4 to 12.

REFERENCES

[1] P. Bergveld, "Development of an Ion-Sensitive Solid-State Device for Neurophysiological Measurements," *IEEE Trans. Biomed. Eng.*, Vol. BME-17, No. 1, pp. 70-71, 1970.

[2] B.-K. Sohn and C.-S. Kim, "A new pH-ISFET based dissolved oxygen sensor by employing electrolysis of oxygen," *Sens. Actuators, B,* Vol. 34, No. 1-3, pp. 435-440, 1996.

[3] B.-K. Sohn, B.-W. Cho, C.-S. Kim, and D.-H. Kwon, "ISFET glucose and sucrose sensors by using platinum electrode and photo-crosslinkable polymers," *Sens. Actuators, B,* Vol. 41, No. 1-3, pp. 7-11, 1997.

[4] L.-S. Park, Y.-J. Hur, and B.-K. Sohn, "Effect of membrane structure on the performance of field-effect transistor potassium-sensitive sensor," *Sens. Actuators, A,* Vol. 57, No. 3, pp. 239-243, 1996.

[5] P. Bergveld, "Thirty years of ISFETOLOGY: What happened in the past 30 years and what may happen in the next 30 years," *Sens. Actuators, B,* Vol. 88, No. 1, pp. 1-20, 2003.

[6] M. J. Schöning, and A. Poghossian, "Recent advances in biologically sensitive field-effect transistors (BioFETs)," *Analyst*, Vol. 127, No. 9, pp. 1137-1151, 2002.

[7] V. Pachauri and S. Ingebrandt, "Biologically sensitive field-effect transistors: from ISFETs to NanoFETs," *Essays Biochem.,* Vol. 60, No. 1, pp. 81-90, 2016.

[8] M. Kaisti, "Detection principles of biological and chemical FET sensors," *Biosens. Bioelectron.,* Vol. 98, pp. 437-448, 2017.

[9] K. B. Parizi, X. Xu, A. Pal, X. Hu, and H. S. P. Wong, "ISFET pH Sensitivity: Counter-Ions Play a Key Role," *Sci. Rep.,* Vol. 7, pp. 41305(1)-41305(10), 2017.

[10] S.-K. Lee, Y.-S. Sohn, and S.-Y. Choi, "Fabrication and characteristics of MOSFET type protein sensor using extended gate," *J. Sens. Sci. Techol.,* Vol. 16, No. 2, pp. 104-109, 2007.

[11] Y. Cui, Q. Wei, H. Park, and C. M. Lieber, "Nanowire nanosensors for highly sensitive and selective detection of biological and chemical species," *Science*, Vol. 293, No. 5533, pp. 1289-1292, 2001.

[12] E. Stern, J. F. Klemic, D. A. Routenberg, P. N. Wyrembak, D. B. Turner-Evans, A. D. Hamilton, D. A. LaVan, T. M. Fahmy, and M. A. Reed, "Label-free immunodetection with CMOS-compatible semiconducting nanowires," *Nature*, Vol. 445, pp. 519-522, 2007.

[13] S. Xu, C. Zhang, S. Jiang, G. Hu, X. Li, Y. Zou, H. Liu, J. Li, Z. Li, X. Wang, M. Li, and J. Wang, "Graphene foam field-effect transistor for ultra-sensitive label-free detection of ATP," *Sens. Actuators, B,* Vol. 284, pp. 125-133, 2019.

[14] X. Lu, M. Mohedano, C. Blawert, E. Matykina, R. Arrabal, K. U. Kainer, and M. L. Zheludkevich, "Plasma electrolytic oxidation coatings with particle additions – A review," *Surf. Coat. Technol.,* Vol. 307-C, pp. 1165-1182, 2016.

[15] Z. Yao, Y. Jiang, F. Jia, Z. Jiang, and F. Wang, "Growth characteristics of plasma electrolytic oxidation ceramic coatings on Ti–6Al–4V alloy," *Appl. Surf. Sci.,* Vol. 254, No. 13, pp. 4084-4091, 2008.

[16] X. Lu, C. Blawert, K. U. Kainer, T. Zhang, F. Wang, and M. L. Zheludkevich, "Influence of particle additions on corrosion and wear resistance of plasma electrolytic oxidation coatings on Mg alloy," *Surf. Coat. Technol.,* Vol. 352, pp. 1-14, 2018.

[17] A. L. Yerokhin, X. Nie, A. Leyland, and A. Matthews, "Characterisation of oxide films produced by plasma electrolytic oxidation of a Ti-6Al-4V alloy," *Surf. Coat. Technol.,* Vol. 130, No. 2-3, pp. 195-206, 2000.

[18] K. Gangwar, and M. Ramulu, "Friction stir welding of titanium alloys: A review," *Mater. Des.,* Vol. 141, pp. 230-255, 2018.

[19] S. Aliasghari, P. Skeldon, and G.E. Thompson, "Plasma electrolytic oxidation of titanium in a phosphate/silicate-electrolyte and tribological performance of the coatings," *Appl. Surf. Sci.,* Vol. 316, pp. 463-476, 2014.

[20] R. R. Boyer, "An overview on the use of titanium in the aerospace industry," *Mater. Sci. Eng., A*, Vol. 213, No. 1-2, pp. 103-114, 1996.

[21] W. Bunjongpru, A. Sungthong, S. Porntheeraphat, Y. Rayanasukha, A. Pankiew, W. Jeamsaksiri, A. Srisuwan, W. Chaisriratanakul, E. Chaowicharat, N. Klunngien, C. Hruanun, A. Poyai, and J. Nukeaw, "Very low drift and high sensitivity of nanocrystal-TiO2 sensing membrane on pH-ISFET fabricated by CMOS compatible process," *Appl. Surf. Sci.,* Vol. 267, pp. 206-211, 2013.

[22] B. G. Streetman, and S. K. Banerjee, *Solid State Electronic Devices, 6th Ed.*, Pearson Prentice Hall, Upper Saddle River, NJ, pp. 283-285, 2006.